JAERI-M
83-240

ATOMIC STRUCTURE CALCULATION OF ENERGY LEVELS AND OSCILLATOR STRENGTHS IN Fe ION, I

(3s-3p and 3p-3d transitions in Fe XV)

January 1984

Keishi ISHII*, Hirotaka KUBO* and Kunio OZAWA

日本原子力研究所
Japan Atomic Energy Research Institute

JAERI-M レポートは，日本原子力研究所が不定期に公刊している研究報告書です。
入手の問合わせは，日本原子力研究所技術情報部情報資料課（〒319—11 茨城県那珂郡東海村）あて，お申しこしください。なお，このほかに財団法人原子力弘済会資料センター（〒319—11 茨城県那珂郡東海村日本原子力研究所内）で複写による実費頒布をおこなっております。

JAERI-M reports are issued irregularly.
Inquiries about availability of the reports should be addressed to Information Section, Division of Technical Information, Japan Atomic Energy Research Institute, Tokai-mura, Naka-gun, Ibaraki-ken 319—11, Japan.

編集兼発行　日本原子力研究所
印　　刷　日立高速印刷株式会社

JAERI-M 83-240

Atomic Structure Calculation of Energy Levels and Oscillator Strengths in Fe Ion, I
(3s - 3p and 3p - 3d transitions in Fe XV)

Keishi ISHII*, Hirotaka KUBO* and Kunio OZAWA

Department of Physics, Tokai Research Establishnent, JAERI

(Received December 24, 1983)

Energy levels and oscillator strengths were calculated for 3s-3p and 3p-3d transition arrays in Fe XV, isoelectronic to Mg I. The energy levels are obtained by the Slater-Condon theory of atomic structure, including explicitly the strong configuration interactions. The calculated wavelengths are presented for electric dipole transition with $gf \geqq 0.0001$. The calculated energy levels are given in diagrams, too. The theoretical spectra are also shown in graphical representation, where the gf is plotted as a function of the wavelength. The results are compared with experimental data, where available.

Keywords: Fe, Highly Ionized Atom, Wavelength, Energy Level, Oscillator Strength, Plasma Diagnostic

---

One of the authors(K.I.) is supported by a co-operative research contract of JAERI with Kyoto University in 1983 fiscal year.

* Department of Engineering Science, Kyoto University, Kyoto 606.

Feイオンのエネルギー準位と振動子強度の原子構造計算，I
（Fe XVイオンの3s －3p及び3p －3d 遷移）

日本原子力研究所東海研究所物理部
石井　慶之*・久保　博孝*・小沢　国夫

（１９８３年１２月２４日受理）

核融合プラズマにおける不純物問題解明のために必要とされる金属イオンの分光学的データに関する研究の一環として，FeXVのエネルギー準位及び$\Delta n = 0$, $n = 3 - 3$遷移の波長と振動子強度の理論計算を行った。計算にはHartree - XR 波動関数とSlater-Condon理論に基づいたCowanプログラムを用いた。結果は表及び図としてまとめた。文献調査による実験値は参考として表中に示した。

本報告は昭和58年度日本原子力研究所との協力研究の成果の一部である。

＊京都大学工学部物理工学教室　京都市左京区吉田本町

Contents

目　　次

§ 1. INTRODUCTION

Knowledge of atomic structure in multiply charged ions of metals is important in the interpretation of spectral data from high temperature plasma. The allowed $\Delta n=0$, $n=2-2$ transitions of $2s^2 2p^q - 2s2p^{q+1}$ and $2s2p^{q+1} - 2p^{q+2}$ types in highly ionized atoms have been widely studied. The energy level data have been compiled and published by Fawcett[1], and the data for oscillator strengths and the lifetimes are also available[2-5]. These data are now well established for the ions with $Z \leqq 28$. The exception is the f-values for some transitions.

The data, however, on the energy levels of M-shell are not yet established. Little is known for oscillator strengths[2,6]. The wavelengths for $\Delta n=0$, $n=3-3$ transitions have been presented by Fawcett[7] again.

The Fe XV, a member of Mg I isoelectronic sequence ,have two electrons outside closed shell, which give rise to singlets and triplets. This spectrum has been studied first by Edlén[8] in 1936, and then by Fawcett & Peacock[9], by Fawcett[10]. Intercombination line, $3s^2\ {}^1S_0 - 3s3p\ {}^3P_1$, was not observed in the above works. Cowan and Widing[11] identified thirteen Fe XV lines in solar flare sprctra by comparision with the calculated wavelengths and the predicted relative intensities. The resonance intersystem line at 417.24Å was confirmed.

Following the previous work on Ti IX[13], Ti X[14] and Ti XI[15], the atomic structure calculation has been extended to Fe XV, using again the program developed by Cowan[16-18]. The energy levels have been obtained based on the Slater-Condon theory for $3s^2$, $3s3p$, $3p^2$, $3s3d$ and $3p3d$ configurations, including explicitly the

configuration interactions. The wavelengths and the weighted oscillator strengths (gf-values) have been calculated for 3s-3p and 3p-3d transitions. The results are given both in numerical tables and in the graphical representations. The calculated spectra are generated in such that the gf-value is plotted against wavelength. They will provide a helpful guidance for finding the missing lines, together with the numerical tables.

§ 2. METHOD OF CALCULATION

The method of calculation used in the present work is the same as in the previous ones[13,14,15], and it is described in some detail there. The full explanation is given by Bromage[19] and Cowan[20]. Therefore only a short description is repeated here. The calculation consists of the following three steps:

(i) calculation of radial integrals, such as E_{av}, F^k, G^k, ζ_{nl} and R^k by the *ab initio* Hartree-XR wavefunctions,

(ii) optimization of the above integrals so as to minimize the discrepancy between the observed and calculated energy levels,

(iii) calculation of wavelengths and oscillator strengths by adopting the scaled radial integrals obtained in the step (ii).

The steps (i) and (ii) were performed separately for the following two configuration groups according to the parity:

1st parity $3s^2$ (①), $3p^2$ (②) and 3s3d(③)

2nd parity 3s3p(①) and 3p3d(②)

The electric dipole radial integrals were also computed by the same Hartree-XR wavefunctions, and used in the step (iii)

configuration interactions. The wavelengths and the weighted oscillator strengths (gf-values) have been calculated for 3s–3p and 3p–3d transitions. The results are given both in numerical tables and in the graphical representations. The calculated spectra are generated in such that the gf-value is plotted against wavelength. They will provide a helpful guidance for finding the missing lines, together with the numerical tables.

§ 2. METHOD OF CALCULATION

The method of calculation used in the present work is the same as in the previous ones[13,14,15], and it is described in some detail there. The full explanation is given by Bromage[19] and Cowan[20]. Therefore only a short description is repeated here. The calculation consists of the following three steps:

(i) calculation of radial integrals, such as E_{av}, F^k, G^k, ζ_{nl} and R^k by the *ab initio* Hartree–XR wavefunctions,

(ii) optimization of the above integrals so as to minimize the discrepancy between the observed and calculated energy levels,

(iii) calculation of wavelengths and oscillator strengths by adopting the scaled radial integrals obtained in the step (ii).

The steps (i) and (ii) were performed separately for the following two configuration groups according to the parity:

1st parity $3s^2$ (①), $3p^2$ (⑧) and 3s3d(⑩)

2nd parity 3s3p(①) and 3p3d(⑧)

The electric dipole radial integrals were also computed by the same Hartree–XR wavefunctions, and used in the step (iii)

calculation.

§ 3. RESULTS

The first step calculation gives the *ab initio* values of the single configuration integrals and configuration interaction integrals as shown in the second column "HXR" of Tables 1 and 3. In the second step calculation, the optimization was reduced to manageable size by fixing ratio of F^k, G^k, ζ and R^k in each integrals[21-23], when necessary. The accuracy of the optimization was measured by a root mean square deviation (Δ) and/or a standard deviation (σ), defined as

$$\Delta = \left[\sum_i (E_{calc}(i) - E_{obs}(i))^2 / (N_l - N_p)\right]^{1/2} , \quad (1)$$

$$\sigma = \left[\sum_i (E_{calc}(i) - E_{obs}(i))^2 / N_l\right]^{1/2} , \quad (2)$$

where $E_{calc}(i)$ and $E_{obs}(i)$ are i-th calculated and observed levels, respectively, N_ℓ is the number of observed energy levels and N_p is the number of adjustable parameters. The following five kinds of free parameters were used in the optimization:

one average energy E_{av}
one scale factor for F^k
one scale factor for G^k
one scale factor for ζ
two scale factors for R^k.

calculation.

§ 3. RESULTS

The first step calculation gives the *ab initio* values of the single configuration integrals and configuration interaction integrals as shown in the second column "HXR" of Tables 1 and 3. In the second step calculation, the optimization was reduced to manageable size by fixing ratio of F^k, G^k, ζ and R^k in each integrals[21-23], when necessary. The accuracy of the optimization was measured by a root mean square deviation (Δ) and/or a standard deviation (σ), defined as

$$\Delta = \left[\sum_i (E_{calc}(i) - E_{obs}(i))^2 / (N_l - N_p)\right]^{1/2} , \quad (1)$$

$$\sigma = \left[\sum_i (E_{calc}(i) - E_{obs}(i))^2 / N_l\right]^{1/2} , \quad (2)$$

where $E_{calc}(i)$ and $E_{obs}(i)$ are i-th calculated and observed levels, respectively, N_ℓ is the number of observed energy levels and N_p is the number of adjustable parameters. The following five kinds of free parameters were used in the optimization:

one average energy E_{av}
one scale factor for F^k
one scale factor for G^k
one scale factor for ζ
two scale factors for R^k.

The reduced electric dipole radial integrals obtained from the same *ab initio* HXR wavefunctions were utilized in the step (iii) calculation combined with the second step results. In the following Tables and Figures, we closely maintain the format of our previous work on Ti IX[13], Ti X[14] and Ti XI[15].

3.1 *Configurations* $3s^2$ (𝔄), $3p^2$ (𝔅) *and* 3s3d(ℭ) *of the first parity*

All levels of this parity were observed[11]. The least-squares optimization, however, cannot be satisfactory, when the above all levels are included simultaniously. Therfore, we have omitted the $^1S_0$ level, because the isoelectronic regularity for the energy levels of $^1S_0$ from K VIII to Fe XV is found poorer than for other levels, and because the assingment of this level is tentative as noted in ref. 11. In the least-squares optimization, the single configuration parameters were adjusted first, while R^k integrals were fixed. Then R^k integrals were adjusted by keeping the single configuration parameters fixed. This procedure was repeated several times. The fitted parameter values are given in the column "Fitted", and the ratio of "Fitted" to "HXR". The *rms* deviation Δ is $0.99\times10^3\,cm^{-1}$, which gives 0.007% of total energy range of the configurations (𝔄+𝔅+ℭ).

The calculated and observed energy levels are listed in Table 2 for the $3s^2$, $3p^2$ and 3s3d, together with their differences ("E(C-O)"). The agreement is satisfactory. One exception is $3p^2\ ^1S$, which is excluded in the optimization calculation. The level designation and its percentage compositions in LS-basis are also given. The corresponding energy

level diagram is shown in Fig.1 for $3p^2$ and 3s3d configurations. The percentage compositions are listed from the largest two contributions in the same configuration and one from the other when over about 10%. The average LS-purity is as high as 92%. Hence, the level designation in the column "Term" is given in LS-coupling notation by the most significant component. A pair of levels $3p^2\ ^1D_2$ and $3s3d\ ^1D_2$ are considerably perturbed with strong mutual configuration interaction: $3p^2\ ^1D$ has a 16% $3s3d\ ^1D$ character. One can notice that the appreciable mixing occurs between $^3P_2$ and $^1D_2$ levels in $3p^2$. This singlet-triplet mixing gives appreciable oscillator strength for some intercombination transitions, which is strictly forbidden in pure LS-coupling.

3.2 *Configurations* 3s3p(α) *and* 3p3d(β) *of the second parity*

The least-squares optimization was performed for the 3s3p(α) and 3p3d(β) configurations, in which one singlet and seven triplet levels were included. The energy of the triplet levels were fixed relative to ground level, based on the observed intercombination[12], $3s^2\ ^1S_0 - 3s3p\ ^3P_1$. The *rms* deviation Δ of $0.126\times10^3\ cm^{-1}$ was achieved, which yield 0.015% of total energy level spread of configurations α and β. The Hartree-XR and fitted parameter values are given in Table 3, together with their ratios. The calculated energy levels are given in Table 4, along with the principal percentage compositions in LS-coupling basis. The observed energy levels are also included for comparison, with their difference with the calculated one. The average LS-purity of 3s3p configuration is close to 100%. It should be noted here that the $^3P_1$ level has only a 0.2% $^1P_1$ character and consiquently

the oscillator strength for $3s^2\ ^1S_0$ - $3s3p\ ^3P_1$ transition is small as described in 3.3. Energy level diagram for 3s3p configuration is displayed in Fig.2.

In 3p3d configuration, two pairs of energy levels are strongly mixed one another; 995.018 and 981.385 for J=2 and 993.260 and 981.260 for J=1. The level designation is generally given according to the most significant composition. However, the second pair is the exception, where the second largest composition is adopted as its level designation by considering the smooth connection of energy level diagram as shown in Fig.3. There is a considerable mixing between $^3F_2$ and $^1D_2$ levels. This indicates that some spin-forbidden transitions from 3p3d to ($3s3d + 3p^2$) gain appreciable oscillator strenghth, as will be described in 3.3. The calculated energy levels are displayed graphically in Fig.3.

3.3 *Wavelengths and Oscillator Strengths*

The reduced electric dipole radial integrals (Table 10) were obtained from the *ab initio* Hatree-XR wavefunction, and used in the third step calculation without scaling. The calculated wavelengths and the *gf*-values for $3s^2$ - 3s3p, $3s^2$ - 3p3d, 3s3p - $3p^2$ and 3s3p - 3s3d transition arrays are listed in Table 5, and those for $3p^2$ - 3s3d in Table 6, and 3s3d - 3p3d in Table 7, respectively. In Tables 5-7, the observed wavelengths are included for comparison, with the difference between the calculated and observed ones. The agreement of the calculated wavelengths with the observed ones is excellent. In Table 5, the calculated *gf*-values are also given, together with the values

derived by Wiese and Fuhr[6] for comparison. The agreement is again good. Table 5 shows that the diference between the calculated and observed wavelengths is less than 0.1 Å for all the components of $^3P - {}^3P$ and $^1P - {}^1D$ in $3s3p - 3p^2$ transition. Therefore, the accuracy of the calculated wavelength for two intercombinations, $^3P_2 - {}^1D_2$ and $^3P_1 - {}^1D_2$, may be as accurate as for the allowed transitions described above. These two lines have fairly large gf-value, so that they are likely to be observed at the predicted position within ± 0.1Å . These two lines are indeed observed[11]. Another intercombination predicted at 435.222Å due to $^1P_1 - {}^3P_2$ is expected to be observed with the same accuracy. For a line of $^1P_1 - {}^1S_0$ in $3s3p-3p^2$ transition, the calculated wavelength differs from the observed one[7] by 1.39Å . This is exceptionally large compared with other members. This is solely due to the fact that $3p^2\ {}^1S_0$ was excluded in the least squares optimization of the energy level calculation. As is noted in 3.2, the isoelectronic regularity in energy level of $3p^2$ is poorer than that of other levels. Therefore, we conclude that there are two ways, whereby the identification is completed in this spectrum. First, this line should be examined again along the isoelectronic sequence. Next, if this transition is confirmed as it is now, the model used in the present calculation has to be modified.

The total number of possible electric dipole transitions among the configurations considered in the present work is shwon in Table 8, arranged in decreasing order of wavelength. The listed transitions are limited for $gf \geqq 0.0001$. The theoretical spectrum was generated from Table 10, and shown in Fig.4, where

the gf-values are plotted in a logarithmic scale as a function of wavelength. Twelve lines above 420 Å and one line below 180 Å were excluded. Two line rich regions, 226 - 244 Å and 316 - 334 Å are shown in Figures 5 and 6,respectively, with wavelength scale being expanded ten times as large as in Fig.4. Three Figures 4-6 provide a helpful guidance for identification of missing lines by direct comparison with a recorded spectrogram.

Comparison of the present gf-value with the NBS work[6] , listed in Table 5, is graphically displyed in Fig.7, where $\log(gf)_{\text{Preset}} - \log(gf)_{\text{NBS}}$ is plotted against $\log(gf)_{\text{Present}}$. The area between two broken lines shows agreement within ± 20%.

In Table 9, the calculated lifetimes for the excited configurations are tabulated. Most of the levels have lifetimes of the order of 0.01 nsec, while 3s3p $^3P_{0,2}$ are metastable. It should be noted that 3s3p $^3P_1$ level has long lifetime of 19.7 nsec. Therefore, this level is collisionally destroyed before it decays by radiative transition. This indicates that the resonance intercombination is hardly observed from the ordinary light source, where electron density is usually high. In Table 9, the calculated lifetimes are listed, which may provide practical help for the future beam-foil lifetime measurement.

§ 4. DISCUSSION

The average LS-purity of the first excited configuration of 3s3p is close to 100%, as shown in Table 4. On the other hand, the LS-purity of the levels of 3p3d configuration ranges from 62% to 100%, and the average is 81%. The purity varies from level to

the gf-values are plotted in a logarithmic scale as a function of wavelength. Twelve lines above 420 Å and one line below 180 Å were excluded. Two line rich regions, 226 - 244 Å and 316 - 334 Å are shown in Figures 5 and 6, respectively, with wavelength scale being expanded ten times as large as in Fig.4. Three Figures 4-6 provide a helpful guidance for identification of missing lines by direct comparison with a recorded spectrogram.

Comparison of the present gf-value with the NBS work[6], listed in Table 5, is graphically displyed in Fig.7, where $\log(gf)_{\text{Preset}} - \log(gf)_{\text{NBS}}$ is plotted against $\log(gf)_{\text{Present}}$. The area between two broken lines shows agreement within ± 20%.

In Table 9, the calculated lifetimes for the excited configurations are tabulated. Most of the levels have lifetimes of the order of 0.01 nsec, while 3s3p $^3P_{0,2}$ are metastable. It should be noted that 3s3p $^3P_1$ level has long lifetime of 19.7 nsec. Therefore, this level is collisionally destroyed before it decays by radiative transition. This indicates that the resonance intercombination is hardly observed from the ordinary light source, where electron density is usually high. In Table 9, the calculated lifetimes are listed, which may provide practical help for the future beam-foil lifetime measurement.

§ 4. DISCUSSION

The average LS-purity of the first excited configuration of 3s3p is close to 100%, as shown in Table 4. On the other hand, the LS-purity of the levels of 3p3d configuration ranges from 62% to 100%, and the average is 81%. The purity varies from level to

level in one configuration, and a few level has heavy admixtures from another configuration. In particular, $^3D_1$ and $^3P_1$ are labeled by the second components of their eigenvectors for the reason described in 3.2. In $3p^2$ configuration, the LS-purity of $^3P_0$ and $^3P_1$ is almost 100%, while that of $^3P_2$ is 82%. This gives the reasonable explanation for a difference of the *gf*-values between the present intermediate calculation and "LS-multiplet" one[6], for $3s3p\ ^3P_J - 3p^2\ ^3P_{J'}$ transition in Table 5. In Ekberg's[25] comparison of eregy levels in the Mg I sequence (his Fig 3), the curves for $3s3d\ ^1D_2$ and $3p^2\ ^1D_2$ plotted from data through Ti XI give a smooth extrapolation to the level values in Fe XV reported here. In Tables 6 and 7, one can notice that several lines with fairly large *gf*-value are not yet observed. Some of them are thus expected to be found in the recorded spectrogram. The present calculation, especially the calculated spectra shown in Figures 4-6, may provide helpful guidance for finding these missing lines, although in many cases the apparent line intensity is dependent on conditions of a light source.

The radial energy integrals were adjusted from their *ab initio* Hartree-XR values, while the radial electric dipole integrals were not. Therefore, the *gf*-values of transition between levels, of which at least one is subject to strong configuration interaction, are less accurate. However, the relative *gf*-values are fairly reliable, because the dipole integrals have a very little influence on them. Fuhr *et al.*[6] noted that the *gf*-values in their table need to be replaced by intermediate coupling data. The present calculation meets to this need. The transition probability situation in Fe XV is thus

improved. The absolute *gf*-values can be determined only after the lifetimes are measured. In this context, Table 9 may be helpful for practical purpose of lifetime measurement.

The authors would like to express their sincere thanks to Dr. Robert D. Cowan for making his programs available, and to Dr. Jan O. Ekberg for his kindest help to make MT copies of the programs and for his valuable discussions regarding the application of the program to the present work. They owes their thanks to Drs. Y. Nakai and T. Shirai of Japan Atomic Energy Research Institute for their valuable comments. The present calculation have been carried out by use of the computer FACOM M-380 at the Data Processing Center of Kyoto University.

REFERENCES

1) B.C. Fawcett: "Wavelengths and classifications of emission lines due to $2s^2 2p^n - 2s2p^{n+1}$ and $2s2p^{n+1} - 2p^{n+2}$ transitions, $Z \leqq 28$", Atomic Data and Nuclear Data Tables 16 (1975) 135-164.

2) M.W. Smith and W.L. Wiese: "Graphical representations of systematic trends of atomic oscillator strengths along isoelectronic sequences and new oscillator strengths derived by interpolation", Astrophys. J. Suppl. Ser. 196 (1971) 103-192.

3) K. Ishii: "Systematic trends of oscillator strengths and lifetimes for $\Delta n=0$, $n=2-2$ transitions in multiply charged ions along isoelectronic sequence", U.S.-Japan Seminar on Plasma Spectroscopy, Kyoto (1979) p.54.

4) B.C. Fawcett: "Theoretical oscillator strengths for $2s^2 2p^n - 2s2p^{n+1}$ and $2s2p^{n+1} - 2p^{n+2}$ transitions and for $2s^2 2p^n$ "forbidden" transitions, Be I, B I, C I, N I, O I series, $Z \leqq 26$", Atomic Data and Nuclear Data Tables 22 (1978) 473-489.

5) K.T. Cheng, Y.-K. Kim and J.P. Desclaux: "Electric dipole, quadrupole, and magnetic dipole transition probabilities of ions isoelectronic to the first-row atoms, Li through F", Atomic Data and Nuclear Data Tables 24 (1979) 111-189.

6) J.R. Fuhr, G.A. Martin, W.L. Wiese and S.M. Younger: "Atomic transition probabilities for iron, cobalt, and nickel (a critical compilation of allowed lines)", J. Phys. Chem. Ref. Data 10 (1981) 305-575.

7) B.C. Fawcett: "Wavelengths and classifications of emission lines due to $3s^2 3p^n - 3s3p^{n+1}$ $3s3p^{n+1} - 3s^2 3p^{n-1}3d$ and other n=3-3 transitions", Report ARU-R4, Culham laboratory, UK (1971).

8) B. Edlén: "Mg I-ähnlich Spektren der Elementen Titan bis Cobalt, Ti XI, V XII, Cr XIII, Mn XIV, Fe XV and Co XVI", Z. Physik 103 (1936) 536-541.

9) B.C. Fawcett and N.J. Peacock: "Highly ionized spectra of the transiton elements", Proc. Phys. Soc. 91 (1967) 973-975.

10) B.C. Fawcett: "Classification of the lower lying energy levels of highly ionized transition elements", J. Phys. B3 (1970) 1732-1741.

11) R.D. Cowan and K.G. Widing: "The extreme-ultraviolet spectrum of Fe XV in a solar flare", Astrophys. J. 180 (1973) 285-292.

12) M. Finkenthal, R.E. Bell and H.W. Moos: "Intercombination lines in Mg I-like Ti XI, V XII, Cr XIII and Fe XV spectra obtained from tokamak plasma", Phys. Lett. 88A (1982) 165-168.

13) K. Ishii: "Atomic structure calculation of energy levels and oscillator strengths in Ti ion. (I. 3s-3p and 3p-3d transitions in Ti IX.)", JAERI-M 83-155 (Report of Japan Atomic Energy Research Institute, 1983).

14) K. Ishii: "Atomic structure calculation of energy levels and oscillator strengths in Ti ion. (II. 3s-3p and 3p-3d transitions in Ti X.)", JAERI-M 83-164 (Report of Japan Atomic Energy Research Institute, 1983).

15) K. Ishii: "Atomic structure calculation of energy levels and oscillator strengths in Ti ion. (III. 3s-3p and 3p-3d transitions in Ti XI.)", JAERI-M 83-198 (Report of Japan

Atomic Energy Research Institute, 1983).

16) R.D. Cowan: "Atomic self-consistent-field calculations using statistical approximations for exchange and correlation", Phys. Rev. **163** (1967) 54-61.

17) R.D. Cowan and D.C. Griffin: "Approximate relativistic corrections to atomic radial wavefunctions", J. Opt. Soc. Am. **66** (1976) 1010-1014.

18) R.D. Cowan: "Theoretical calculation of atomic spectra using digital computers", J. Opt. Soc. Am. **58** (1968) 808-818, and "Theoretical study of $p^m - p^{m-1}\ell$ spectra", *ibid.* **58** (1968) 924-933.

19) G.E. Bromage: "The Cowan-Zealot-Suite of computer programs for atomic structure", Report **AL-R-3**, Appleton Laboratory, UK (1978).

20) R.D. Cowan: *The Theory of Atomic Structure and Spectra* (Univ. Calif. Press, Berkley, 1981).

21) G.E. Bromage, R.D. Cowan and B.C. Fawcett: "Energy levels and oscillator strengths for $3s^2 3p^n - 3s^2 3p^{n-1} 3d$ transitions of Fe X and Fe XI", Physica Scripta **15** (1977) 177-182.

22) G.E. Bromage, R.D. Cowan and B.C. Fawcett: "Atomic structure calculations involving optimization of radial integrals: Energy levels and oscillator strengths for Fe XII and Fe XIII 3p-3d and 3s-3p transitions", Mon. Not. R. astr. Soc. **183** (1978) 19-28.

23) G.E. Bromage: "Atomic structure calculations: Energy levels and oscillator strengths for 3s-3p and 3p-3d transitions in nickel XII to XV and vanadium VII to X spectra", Astron. Astrophys. Suppl. Ser. **41** (1980) 79-83.

24) R.L. Kelly and L.J. Palumbo : "Atomic and ionic emission lines below 2000 angstrom. Hydrogen through krypton", NRL-7599 (1973) 299-321.

25) J.O. Ekberg: "Analysis of the Mg-I like spectra K VIII, Ca IX, Sc X and Ti XI", Physica Scripta 4 (1971) 101-109.

ADDENDA

Present calculation of Fe XV was carried out as an extension of the previous work on Ti IX ,Ti X and Ti XI. After the completion of the present work, Fawcett [1,2] publisshed the same calculation on Fe XV. While we were concentrated on Ti and Fe, he presented systematic calculation of Al-like ions from Cl V to Ni XVI and Mg-like ions from S V to Ni XVII. The present results are in agreement with ref.[2] . However, when compared with the observed data, the present results show better agreement. We present here the wavelengths and gf-values for forbidden lines in addition to that for allowed ones. The graphical representations are also diaplayed.

[1] B.C. Fawcett :"Calculated oscillator strenghts and wavelengths for allowed transitions within the third shell for ions in the Al-like isoelectronic sequence between Cl V and Ni XVI", Atomic Data and Nuclear Data Tables 28 (1983) 557-578.

[2] B.C. Fawcett :"Calculated oscillator strenghts and wavelengths for allowed transitions within the third shell for ions in the Mg-like isoelectronic sequence between S V and Ni XVII", Atomic Data and Nuclear Data Tables 28 (1983) 579-596.

Table 1 Parameter values (in $10^3\,cm^{-1}$) for $3s^2$, $3p^2$ and 3s3d configurations in Fe XV. Ratio is defined as Fitted/HXR.

Parameters	Hartree-XR	Fitted	Ratio	C.I.
$E_{av}(3s^2)$	0.000	5.804	-----	
$E_{av}(3p^2)$	575.314	587.083	1.020	
$F^2(3p,3p)$	147.419	131.947	0.895	
$\zeta(3p)$	14.328	13.303	.928	
$E_{av}(3s,3d)$	679.212	690.929	1.017	
$\zeta(3d)$	1.497	1.040	0.695	
$G^2(3s,3d)$	126.421	105.606	0.835	
$R^1(ss,pp)$	190.176	106.393	0.599	$3s^2 * 3p^2$
$R^1(pp,sd)$	172.202	153.350	0.891	$3p^2 * 3s3d$
Δ		0.99 *		
σ		0.44		

*Number of free parameter is 7.

Table 2 Calculated and observed energy levels (in $10^3\,cm^{-1}$) for $3s^2$, $3p^2$ and 3s3d configurations in Fe XV.

Conf	Term	J	E(calc)	E(obs)	E(C-O)*	Percentage Composition
$3s^2$	^1S	0	0.00	0.000	0.00	99%
$3p^2$	^3P	2	581.700	581.701[a]	-0.001	82%, 13% ^1D
	^3P	1	564.598	564.597[a]	0.001	100%
	^3P	0	554.503	544.505[a]	-0.002	97%
	^1D	2	559.606	559.606[a]	0.000	67%, 18% ^3P, 16% 3s3d ^1D
	^1S	0	659.667	660.984[b]	-1.317†	96%
3s3d	^3D	3	681.408	681.432[a]	-0.024	100%
	^3D	2	679.835	679.775[a]	0.060	100%
	^3D	1	678.808	678.844[a]	-0.036	100%
	^1D	2	762.135	762.135[a]	0.000	80%, 19% $3p^2$ ^1D

[a] Cowan and Widing (1973), ref.11).
[b] Fawcett (1971), ref.7).
† See text for detail.

Table 3 Parameter values (in $10^3\,cm^{-1}$) for 3s3p and 3p3d configurations in Fe XV. Ratio is defined as Fitted/HXR.

Parameters	Hartree-XR	Fitted	Ratio	C.I.
E_{av}(3s3p)	261.225	277.614	1.063	
ζ(3p)	14.393	13.328	0.926	
G^1(3s,3p)	190.685	172.501	0.905	
E_{av}(3p3d)	970.011	981.148	1.011	
ζ(3p)	14.321	13.261	0.926	
ζ(3d)	1.494	1.271	0.851	
F^2(3p,3d)	147.977	125.403	0.847	
G^1(3p,3d)	164.355	148.682	0.905	
G^3(3p,3d)	108.538	98.188	0.905	
R^1(sp,pd)	172.490	137.992	0.800	3s3p * 3p3d
R^2(sp,pd)	130.904	104.723	0.800	3s3p * 3p3d
Δ		0.126*		
σ		0.048		

* Number of free parameter is 6.

Table 4 Calculated and observed energy levels (in $10^3\,cm^{-1}$) for 3s3p and 3p3d configurations in Fe XV.

Conf	Term	J	E(calc)	E(obs)	E(C-O)*	% Composition
3s3p	^{3}P	2	253.809	253.826[a]	-0.017	100%
	^{3}P	1	239.733	239.663[a]	0.070	100%
	^{3}P	0	233.875	233.928[a]	-0.103	100%
	^{1}P	1	351.932	351.932[a]	0.000	98%
3p3d	^{3}F	4	949.660	949.660[b]	0.000	100%
	^{3}F	3	938.190	938.190[b]	0.000	99%
	^{3}F	2	928.451	928.450[b]	0.001	89%, 11% ^{1}D
	^{3}D	3	994.940			98%
	^{3}D	2	995.018			66%, 33% ^{3}P
	^{3}D	1	993.260			37%, 63% ^{3}P
	^{3}P	2	981.385			63%, 32% ^{3}D
	^{3}P	1	981.260			36%, 62% ^{3}D
	^{3}P	0	991.572			100%
	^{1}F	3	1063.879			99%
	^{1}D	2	949.657			84%, 10% ^{3}F
	^{1}P	1	1069.544			97%

[a,b] See footnote in Table 3.

Table 5 Calculated and observed wavelengths for $3s^2$ – 3s3p, $3s^2$ – 3p3d, 3s3p – $3p^2$ and 3s3p – 3s3d transition arrays in Fe XV, with calculated weighted oscillator strengths.

Transition			Wavelength (in A)				
Conf	Term	J–J	Calc	Obs	C–O	gf	gf^*
$3s^2$ –3s3p	^1S–^1P	0–1	284.146	284.146[a]	0.000	0.8611	0.80
	^1S–^3P	0–1	417.130	417.24[a]	–0.11	0.0040	0.0044
$3s^2$ –3p3d	^1S–^1P	0–1	93.498			0.0093	
3s3p–$3p^2$	^3P–^3P	2–2	304.979	305.00[b]	–0.02	0.8762	0.885
	^3P–^3P	1–2	292.426	292.36[b]	0.07	0.2796	0.286
	^3P–^3P	2–1	321.762	321.79[a]	–0.03	0.3363	0.332
				321.761[b]	0.001		
	^3P–^3P	1–1	307.821	307.74[a]	0.08	0.2103	0.209
				307.78[b]	0.04		
	^3P–^3P	1–0	317.693	317.62[b]	0.07	0.2709	0.268
	^3P–^3P	0–1	302.368	302.45[b]	–0.08	0.2874	0.285
	^1P–^1D	1–2	481.524	481.53[a]	0.01	0.2692	0.269
				481.52[b]	0.00		
	^1P–^1S	1–0	324.955	323.57[a]	1.39	0.2693	0.315
	^1P–^3P	1–2	435.222			0.0745	0.066
	^1P–^3P	1–1	470.221			0.0009	0.0008
	^1P–^3P	1–0	493.655			0.0018	0.0023
	^3P–^1D	2–2	327.014	327.03[a]	–0.02	0.1763	0.160
	^3P–^1D	1–2	312.624	312.55[a]	0.07	0.0896	0.081
	^3P–^1S	1–0	238.133			0.0033	
3s3p–3s3d	^3P–^3D	2–3	233.864	233.86[a]	0.00	1.2619	1.370
				233.865[b]	–0.01		
	^3P–^3D	2–2	234.727			0.2260	0.225
	^3P–^3D	1–2	227.220	227.22[a]	0.00	0.6943	0.690
	^3P–^3D	2–1	235.295			0.0150	0.016
	^3P–^3D	1–1	227.752	227.70[b]	0.05	0.2306	0.231
	^3P–^3D	0–1	224.753	224.76[a]	–0.01	0.3137	0.314
				224.745[b]	0.008		
	^1P–^1D	1–2	243.782	243.782[a]	0.000	1.8612	1.869
				243.783[b]	–0.001		
	^1P–^3D	1–2	304.968			0.0017	0.0010
	^1P–^3D	1–1	305.926			0.0012	0.0010
	^3P–^1D	2–2	196.724			0.0005	0.0003
	^3P–^1D	1–2	191.423			0.0102	0.0084

[a] Cowan *et al.*, (1973), ref.11).
[b] Fawcett (1971), ref.7).
* Fuhr *et al.*, (1981), ref.6).
† See text for detail.

Table 6 Calculated and observed wavelengths for $3p^2$ - 3p3d transition in Fe XV, with calculated weighted oscillator strengths.

Transition		Wavelength (in Å)				
Term	J-J	Calc	Obs	C-O	gf	gf^*
$^3P-^3F$	2-3	280.512			0.0108	
$^3P-^3F$	2-2	288.391			0.0073	
$^3P-^3F$	1-2	274.836			0.0020	
$^3P-^3D$	2-3	241.990			1.5437	
$^3P-^3D$	2-2	241.945			0.7982	
$^3P-^3D$	1-2	232.331			0.3337	
$^3P-^3D$	2-1	242.978			0.1831	
$^3P-^3D$	1-1	233.284			0.4456	
$^3P-^3D$	0-1	227.916			0.0068	
$^3P-^3P$	2-2	250.197			0.1416	
$^3P-^3P$	1-2	239.930			0.9375	
$^3P-^3P$	2-1	250.275			0.0244	
$^3P-^3P$	1-1	240.003			0.0611	
$^3P-^3P$	0-1	234.325	234.79[a]	-0.46	0.6708	
$^3P-^3P$	1-0	234.206			0.1874	
$^1D-^1F$	2-3	198.305			0.8169	1.16
$^1D-^1D$	2-2	256.376			0.7924	
$^1D-^1P$	2-1	196.102			0.0047	
$^1S-^1P$	0-1	243.976			0.7620	
$^1D-^3F$	2-2	271.116			0.1048	
$^1D-^3F$	2-3	264.142			0.0118	
$^1D-^3D$	2-3	229.709			0.4467	
$^1D-^3D$	2-2	229.668			0.1342	
$^1D-^3D$	2-1	230.598			0.0406	
$^1D-^3P$	2-2	237.091			0.0046	
$^1D-^3P$	2-1	237.161			0.0039	
$^1S-^3P$	0-1	310.952			0.0011	
$^3P-^1F$	2-3	207.392			0.2484	
$^3P-^1D$	2-2	271.770			0.0918	
$^3P-^1D$	1-2	259.700			0.0393	
$^3P-^1P$	2-1	204.983			0.0013	
$^3P-^1P$	1-1	198.041			0.0015	
$^3P-^1P$	0-1	194.159			0.0046	

*Fuhr *et al.*, (1981), ref.6).
Source of observed data: see footnote in Table 5.

Table 7 Calculated and observed wavelengths for 3s3d - 3p3d transition in Fe XV, with calculated weighted oscillator strengths.

Transition		Wavelength (in Å)				
Term	J-J	Calc	Obs	C-O	gf	gf*
$^3D-^3F$					2.467†	2.265†
$^3D-^3F$	3-4	372.784	372.78[b]	0.00	1.1187	
$^3D-^3F$	3-3	389.435			0.1539	
$^3D-^3F$	2-3	387.064	387.00[b]	0.06	0.6787	
$^3D-^3F$	3-2	404.788			0.0017	
$^3D-^3F$	2-2	402.227			0.1099	
$^3D-^3F$	1-2	400.572	400.65[b]	-0.08	0.4037	
$^3D-^3D$	3-3	318.947			0.8204	
$^3D-^3D$	2-3	317.354			0.1922	
$^3D-^3D$	3-2	318.868			0.0425	
$^3D-^3D$	2-2	317.276			0.5837	
$^3D-^3D$	1-2	316.246			0.1332	
$^3D-^3D$	2-1	319.055			0.0781	
$^3D-^3D$	1-1	318.013			0.3921	
$^3D-^3P$	3-2	333.358			0.6790	
$^3D-^3P$	2-2	331.619			0.0093	
$^3D-^3P$	1-2	330.494			0.0315	
$^3D-^3P$	2-1	331.758			0.3783	
$^3D-^3P$	1-1	330.631			0.0550	
$^3D-^3P$	1-0	319.729			0.1625	
$^1D-^1F$	2-3	331.407			2.2544	1.89
$^1D-^1D$	2-2	533.270			0.1256	
$^1D-^1P$	2-1	325.300			0.6612	
$^1D-^3F$	2-3	568.005			0.0048	
$^1D-^3F$	2-2	601.266			0.0135	
$^1D-^3D$	2-3	429.544			0.0052	
$^1D-^3D$	2-1	432.666			0.0003	
$^1D-^3P$	2-2	456.100			0.0065	
$^1D-^3P$	2-2	429.401			0.0002	
$^1D-^3P$	2-1	456.362			0.0058	
$^3D-^1F$	3-3	261.458			0.0106	
$^3D-^1F$	2-3	260.387			0.0021	
$^3D-^1D$	3-2	372.787			0.0421	
$^3D-^1D$	2-2	370.614			0.0104	
$^3D-^1D$	1-2	369.209			0.0480	
$^3D-^1P$	2-1	256.602			0.0052	
$^3D-^1P$	1-1	255.927			0.0014	

*Fuhr *et al.*, (1981), ref.6).
†Multilet sum.
Source of observed data: see footnote in Table 5.

Table 8 Calculated and observed wavelengths for transitions between ($3s^2$ + $3p^2$ + 3s3d) and (3s3p + 3p3d) configurations with calculated *gf*-value in Fe XV. Arranged in order of decreasing wavelength.

No	Transitin Energy (10^3 cm^{-1})	Conf	Term	J-J	Wavelength(Å) Calc	Obs	*gf*
1	762.135- 928.451	3s3d-3p3d	$^1D-^3F$	2-2	601.266		0.0135
2	762.135- 938.190	3s3d-3p3d	$^1D-^3F$	2-3	568.005		0.0048
3	762.135- 949.657	3s3d-3p3d	$^1D-^1D$	2-2	533.270		0.1256
4	351.932- 554.502	$3s3p-3p^2$	$^1P-^3P$	1-0	493.655		0.0018
5	351.932- 559.605	$3s3p-3p^2$	$^1P-^1D$	1-2	481.524	481.53[a]	0.2692
6	351.932- 564.597	$3s3p-3p^2$	$^1P-^3P$	1-1	470.221		0.0009
7	762.135- 981.259	3s3d-3p3d	$^1D-^3P$	2-1	456.362		0.0058
8	762.135- 981.385	3s3d-3p3d	$^1D-^3P$	2-2	456.100		0.0065
9	351.932- 581.699	$3s3p-3p^2$	$^1P-^3P$	1-2	435.222		0.0745
10	762.135- 993.260	3s3d-3p3d	$^1D-^3D$	2-1	432.666		0.0003
11	762.135- 994.940	3s3d-3p3d	$^1D-^3D$	2-3	429.544		0.0052
12	762.135- 995.017	3s3d-3p3d	$^1D-^3P$	2-2	429.401		0.0002
13	0.000- 239.733	$3s^2$ -3s3p	$^1S-^3P$	0-1	417.130	417.24[a]	0.0040
14	681.408- 928.451	3s3d-3p3d	$^3D-^3F$	3-2	404.788		0.0017
15	679.835- 928.451	3s3d-3p3d	$^3D-^3F$	2-2	402.227		0.1099
16	678.808- 928.451	3s3d-3p3d	$^3D-^3F$	1-2	400.572	400.65[b]	0.4037
17	681.408- 938.190	3s3d-3p3d	$^3D-^3F$	3-3	389.435		0.1539
18	679.835- 938.190	3s3d-3p3d	$^3D-^3F$	2-3	387.064	387.00[b]	0.6787
19	681.408- 949.657	3s3d-3p3d	$^3D-^1D$	3-2	372.787		0.0421
20	681.408- 949.660	3s3d-3p3d	$^3D-^3F$	3-4	372.784	372.78[b]	1.1187
21	679.835- 949.657	3s3d-3p3d	$^3D-^1D$	2-2	370.614		0.0104
22	678.808- 949.657	3s3d-3p3d	$^3D-^1D$	1-2	369.209		0.0480
23	681.408- 981.385	3s3d-3p3d	$^3D-^3P$	3-2	333.358		0.6790
24	679.835- 981.259	3s3d-3p3d	$^3D-^3P$	2-1	331.758		0.3783
25	679.835- 981.385	3s3d-3p3d	$^3D-^3P$	2-2	331.619		0.0093
26	762.135-1063.879	3s3d-3p3d	$^1D-^1F$	2-3	331.407		2.2544
27	678.808- 981.259	3s3d-3p3d	$^3D-^3P$	1-1	330.631		0.0550
28	678.808- 981.385	3s3d-3p3d	$^3D-^3P$	1-2	330.494		0.0315
29	253.809- 559.605	$3s3p-3p^2$	$^3P-^1D$	2-2	327.014	327.03[a]	0.1763
30	762.135-1069.544	3s3d-3p3d	$^1D-^1P$	2-1	325.300		0.6612
31	351.932- 659.667	$3s3p-3p^2$	$^1P-^1S$	1-0	324.955	323.57[a]	0.2693
32	253.809- 564.597	$3s3p-3p^2$	$^3P-^3P$	2-1	321.762	321.79[a]	0.3363
33	678.808- 991.572	3s3d-3p3d	$^3D-^3P$	1-0	319.729		0.1625
34	679.835- 993.260	3s3d-3p3d	$^3D-^3D$	2-1	319.055		0.0781
35	681.408- 994.940	3s3d-3p3d	$^3D-^3D$	3-3	318.947		0.8204
36	681.408- 995.017	3s3d-3p3d	$^3D-^3D$	3-2	318.868		0.0425
37	678.808- 993.260	3s3d-3p3d	$^3D-^3D$	1-1	318.013		0.3921
38	239.733- 554.502	$3s3p-3p^2$	$^3P-^3P$	1-0	317.693	317.62[b]	0.2709
39	679.835- 994.940	3s3d-3p3d	$^3D-^3D$	2-3	317.354		0.1922
40	679.835- 995.017	3s3d-3p3d	$^3D-^3D$	2-2	317.276		0.5837

Table 8 *Continued*

41	678.808– 995.017	$3s3d-3p3d$	$^3D-^3D$	1–2	316.246		0.1332
42	239.733– 559.605	$3s3p-3p^2$	$^3P-^1D$	1–2	312.624	312.55[a]	0.0896
43	659.667– 981.259	$3p^2-3p3d$	$^1S-^3P$	0–1	310.952		0.0011
44	239.733– 564.597	$3s3p-3p^2$	$^3P-^3P$	1–1	307.821	307.74[a]	0.2103
45	351.932– 678.808	$3s3p-3s3d$	$^1P-^3D$	1–1	305.926		0.0012
46	253.809– 581.699	$3s3p-3p^2$	$^3P-^3P$	2–2	304.979	305.00[b]	0.8762
47	351.932– 679.835	$3s3p-3s3d$	$^1P-^3D$	1–2	304.968		0.0017
48	233.875– 564.597	$3s3p-3p^2$	$^3P-^3P$	0–1	302.368	302.45[b]	0.2874
49	239.733– 581.699	$3s3p-3p^2$	$^3P-^3P$	1–2	292.426	292.36[b]	0.2796
50	581.699– 928.451	$3p^2-3p3d$	$^3P-^3F$	2–2	288.391		0.0073
51	0.000– 351.932	$3s^2-3s3p$	$^1S-^1P$	0–1	284.146	284.146[a]	0.8611
52	581.699– 938.190	$3p^2-3p3d$	$^3P-^3F$	2–3	280.512		0.0108
53	564.597– 928.451	$3p^2-3p3d$	$^3P-^3F$	1–2	274.836		0.0020
54	581.699– 949.657	$3p^2-3p3d$	$^3P-^1D$	2–2	271.770		0.0918
55	559.605– 928.451	$3p^2-3p3d$	$^1D-^3F$	2–2	271.116		0.1048
56	559.605– 938.190	$3p^2-3p3d$	$^1D-^3F$	2–3	264.142		0.0118
57	681.408–1063.879	$3s3d-3p3d$	$^3D-^1F$	3–3	261.458		0.0106
58	679.835–1063.879	$3s3d-3p3d$	$^3D-^1F$	2–3	260.387		0.0021
59	564.597– 949.657	$3p^2-3p3d$	$^3P-^1D$	1–2	259.700		0.0393
60	679.835–1069.544	$3s3d-3p3d$	$^3D-^1P$	2–1	256.602		0.0052
61	559.605– 949.657	$3p^2-3p3d$	$^1D-^1D$	2–2	256.376		0.7924
62	678.808–1069.544	$3s3d-3p3d$	$^3D-^1P$	1–1	255.927		0.0014
63	581.699– 981.259	$3p^2-3p3d$	$^3P-^3P$	2–1	250.275		0.0244
64	581.699– 981.385	$3p^2-3p3d$	$^3P-^3P$	2–2	250.197		0.1416
65	659.667–1069.544	$3p^2-3p3d$	$^1S-^1P$	0–1	243.976		0.7620
66	351.932– 762.135	$3s3p-3s3d$	$^1P-^1D$	1–2	243.782	243.782[a]	1.8612
67	581.699– 993.260	$3p^2-3p3d$	$^3P-^3D$	2–1	242.978		0.1831
68	581.699– 994.940	$3p^2-3p3d$	$^3P-^3D$	2–3	241.990		1.5437
69	581.699– 995.017	$3p^2-3p3d$	$^3P-^3D$	2–2	241.945		0.7982
70	564.597– 981.259	$3p^2-3p3d$	$^3P-^3P$	1–1	240.003		0.0611
71	564.597– 981.385	$3p^2-3p3d$	$^3P-^3P$	1–2	239.930		0.9375
72	239.733– 659.667	$3s3p-3p^2$	$^3P-^1S$	1–0	238.133		0.0033
73	559.605– 981.259	$3p^2-3p3d$	$^1D-^3P$	2–1	237.161		0.0039
74	559.605– 981.385	$3p^2-3p3d$	$^1D-^3P$	2–2	237.091		0.0046
75	253.809– 678.808	$3s3p-3s3d$	$^3P-^3D$	2–1	235.295		0.0150
76	253.809– 679.835	$3s3p-3s3d$	$^3P-^3D$	2–2	234.727		0.2260
77	554.502– 981.259	$3p^2-3p3d$	$^3P-^3P$	0–1	234.325	234.79[a]	0.6708
78	564.597– 991.572	$3p^2-3p3d$	$^3P-^3P$	1–0	234.206		0.1874
79	253.809– 681.408	$3s3p-3s3d$	$^3P-^3D$	2–3	233.864	233.86[a]	1.2619
80	564.597– 993.260	$3p^2-3p3d$	$^3P-^3D$	1–1	233.284		0.4456
81	564.597– 995.017	$3p^2-3p3d$	$^3P-^3D$	1–2	232.331		0.3337
82	559.605– 993.260	$3p^2-3p3d$	$^1D-^3D$	2–1	230.598		0.0406
83	559.605– 994.940	$3p^2-3p3d$	$^1D-^3D$	2–3	229.709		0.4467
84	559.605– 995.017	$3p^2-3p3d$	$^1D-^3D$	2–2	229.668		0.1342
85	554.502– 993.260	$3p^2-3p3d$	$^3P-^3D$	0–1	227.916		0.0068
86	239.733– 678.808	$3s3p-3s3d$	$^3P-^3D$	1–1	227.752	227.70[b]	0.2306
87	239.733– 679.835	$3s3p-3s3d$	$^3P-^3D$	1–2	227.220	227.22[a]	0.6943
88	233.875– 678.808	$3s3p-3s3d$	$^3P-^3D$	0–1	224.753	224.76[a]	0.3137
89	581.699–1063.879	$3p^2-3p3d$	$^3P-^1F$	2–3	207.392		0.2484
90	581.699–1069.544	$3p^2-3p3d$	$^3P-^1P$	2–1	204.983		0.0013

Table 8. *Continued*

91	559.605–1063.879	$3p^2$	–3p3d	^1D–^1F	2–3	198.305	0.8169
92	564.597–1069.544	$3p^2$	–3p3d	^3P–^1P	1–1	198.041	0.0015
93	253.809– 762.135	3s3p	–3s3d	^3P–^1D	2–2	196.724	0.0005
94	559.605–1069.544	$3p^2$	–3p3d	^1D–^1P	2–1	196.102	0.0047
95	554.502–1069.544	$3p^2$	–3p3d	^3P–^1P	0–1	194.159	0.0046
96	239.733– 762.135	3s3p	–3s3d	^3P–^1D	1–2	191.423	0.0102
97	0.000–1069.544	$3s^2$	–3p3d	^1S–^1P	0–1	93.498	0.0093

[a] Cowan *et al.*, (1973), ref.11).
[b] Fawcett (1971), ref.7).
[†] See text for detail.

Table 9 Calculated lifetimes (in nsec) for levels of the excited configurations in Fe XV.

Conf	Term	J	Energy	Lifetime*
$3p^2$	^3P	2	581.70	5.73(-2)
	^3P	1	564.60	5.22(-2)
	^3P	0	554.50	5.57(-2)
	^1D	2	559.61	2.01(-1)
	^1S	0	659.67	5.75(-2)
3s3d	^3D	3	681.41	4.55(-2)
	^3D	2	679.84	4.27(-2)
	^3D	1	678.81	4.11(-2)
	^1D	2	762.14	2.37(-2)
3s3p	^3P	2	253.81	----
	^3P	1	239.73	1.97(+1)
	^3P	0	233.88	----
	^1P	1	351.93	4.22(-2)
3p3d	^3F	4	949.66	1.68(-1)
	^3F	3	938.19	1.79(-1)
	^3F	2	928.45	1.57(-1)
	^3D	3	994.94	2.34(-2)
	^3D	2	995.02	2.51(-2)
	^3D	1	981.26	2.54(-2)
	^3P	2	981.39	2.98(-2)
	^3P	1	993.26	2.67(-2)
	^3P	0	991.57	3.00(-2)
	^1F	3	1063.88	2.22(-2)
	^1D	2	949.66	4.98(-2)
	^1P	1	1069.54	2.19(-2)

*Figures in parentheses are the power of 10 by which the preceding number should be multiplied.

Table 10 Calculated reduced electric dipole radial integrals (in atomic units) in Fe XV.

Transition		Reduced E1 integral
$3s^2$	- 3s3p	(3s:R1:3p)= 0.6759
3s3p	- $3p^2$	(3s:R1:3p)=-0.6762
	- 3s3d	(3p:R1:3d)=-0.8671
$3p^2$	- 3p3d	(3p:R1:3d)= 0.8688
3s3d	- 3p3d	(3s:R1:3p)= 0.6765

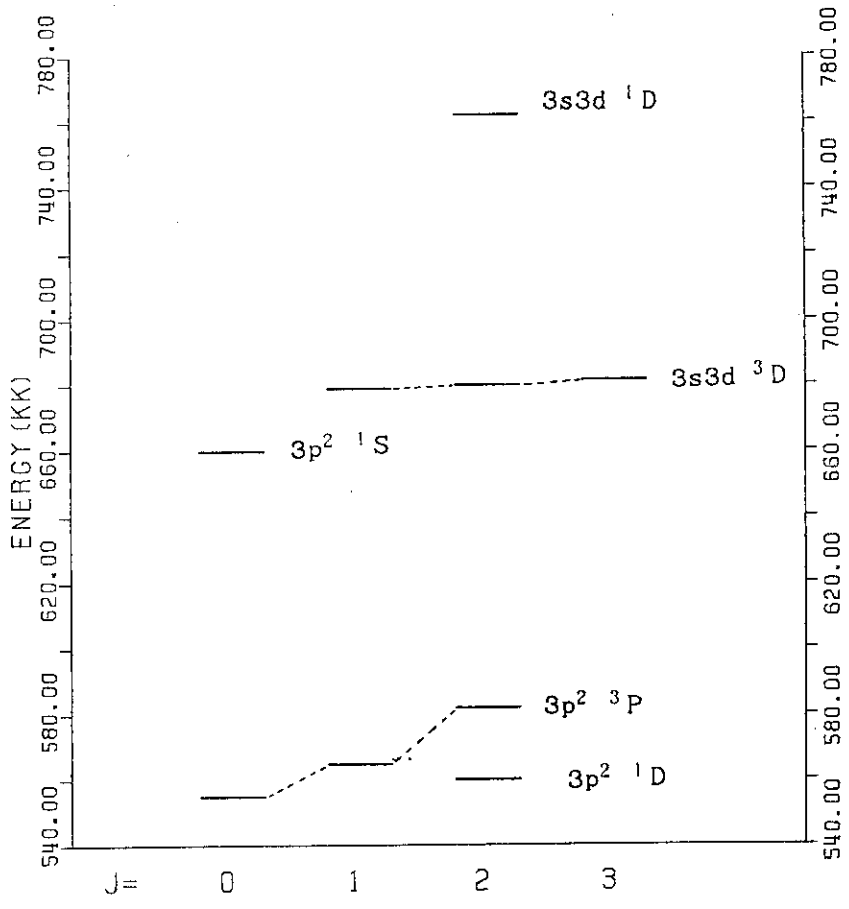

Fig.1 Calculated energy level diagram of $3p^2$ (Ⓑ) and 3s3d (Ⓒ) configurations of the first parity in Fe XV. Energy is in $10^3\,cm^{-1}$.

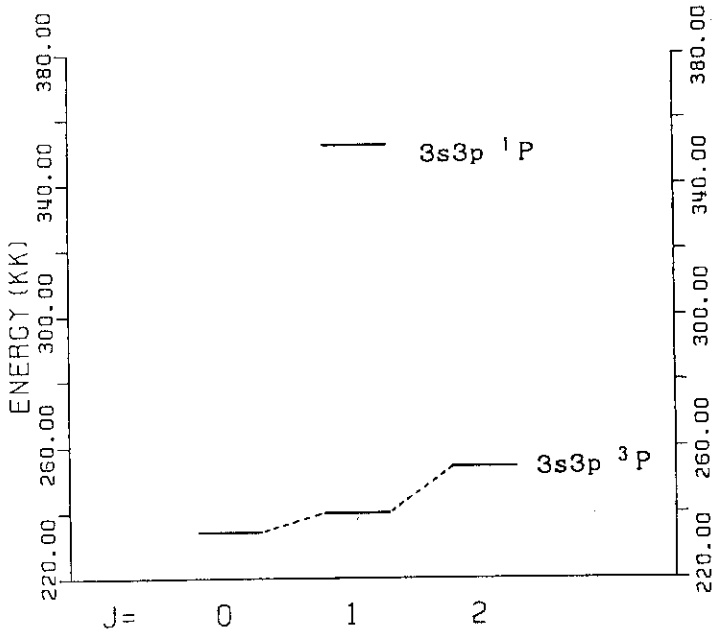

Fig.2 Calculated energy level diagram of 3s3p configuration of the second parity in Fe XV. Energy in $10^3\,cm^{-1}$.

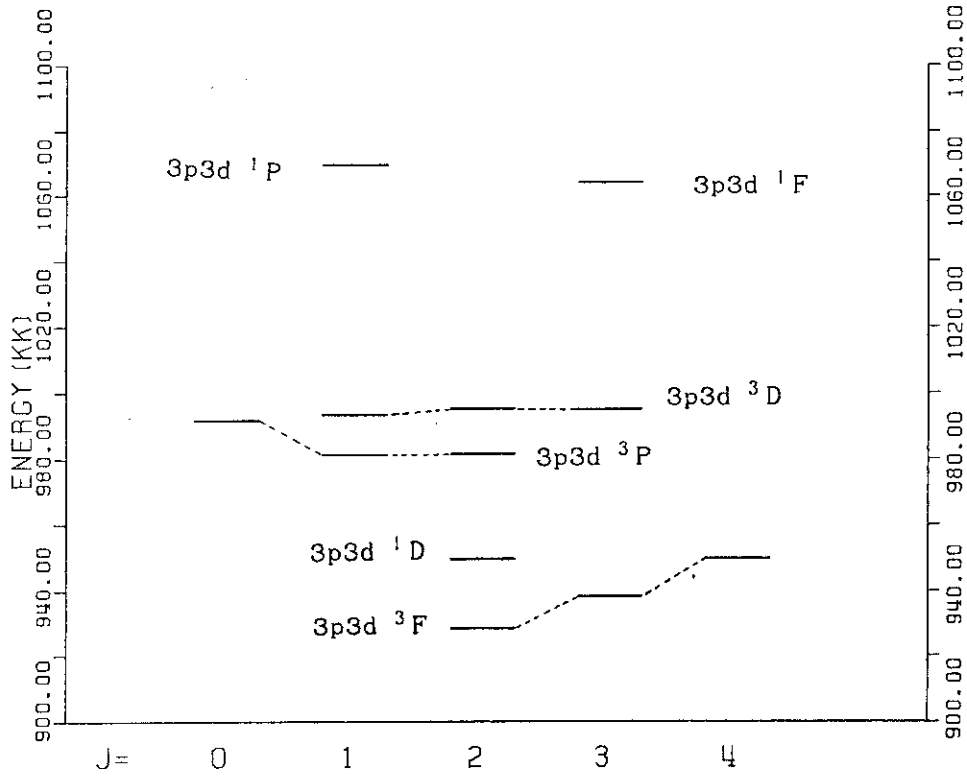

Fig.3 Calculated energy level diagram of 3p3d configuration of the the second parity in Fe XV. Energy in $10^3\,cm^{-1}$.

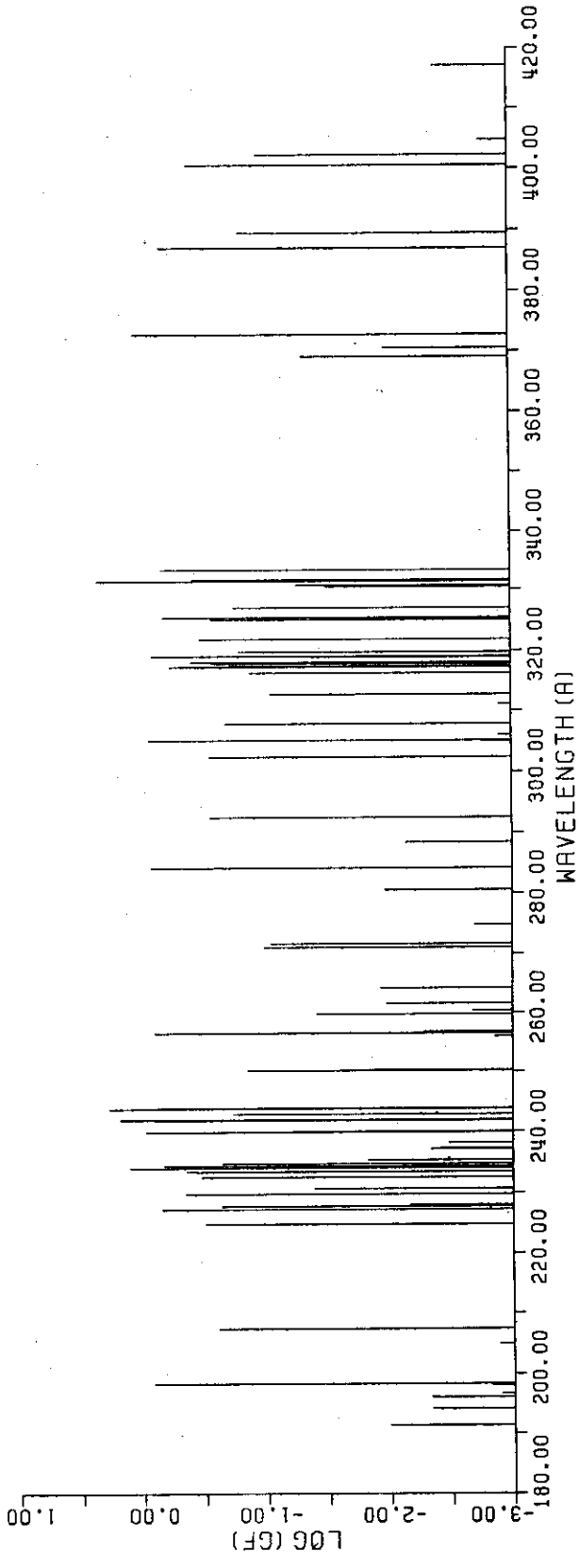

Fig.4 Calculated line pattern for the transitions in Fe XV, reproduced from Table 8.

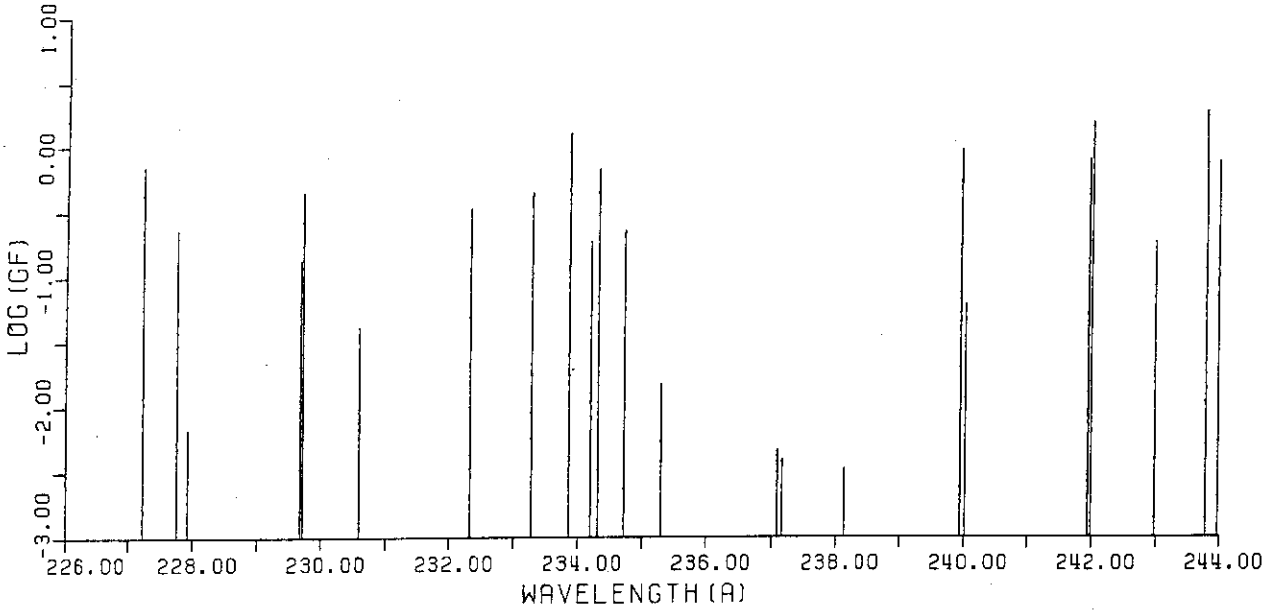

Fig.5 Enlarged partial line pattern in the wavelength range 226 to 244 A .

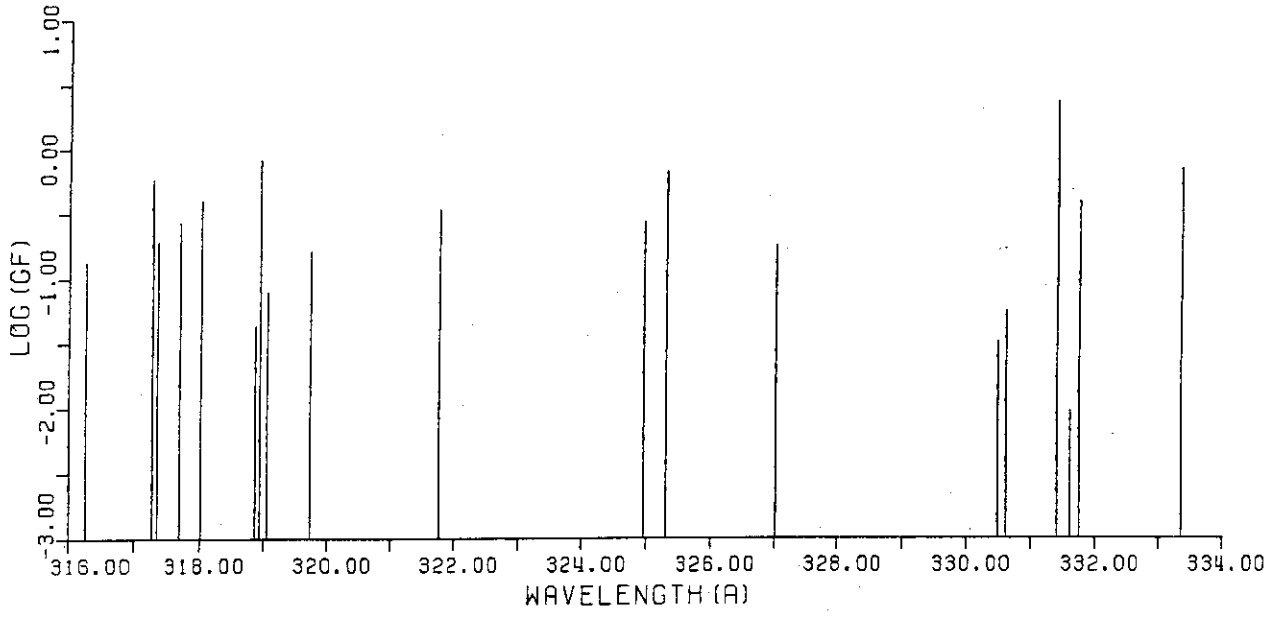

Fig.6 Enlarged partial line pattern in the wavelength range 316 to 334 A .

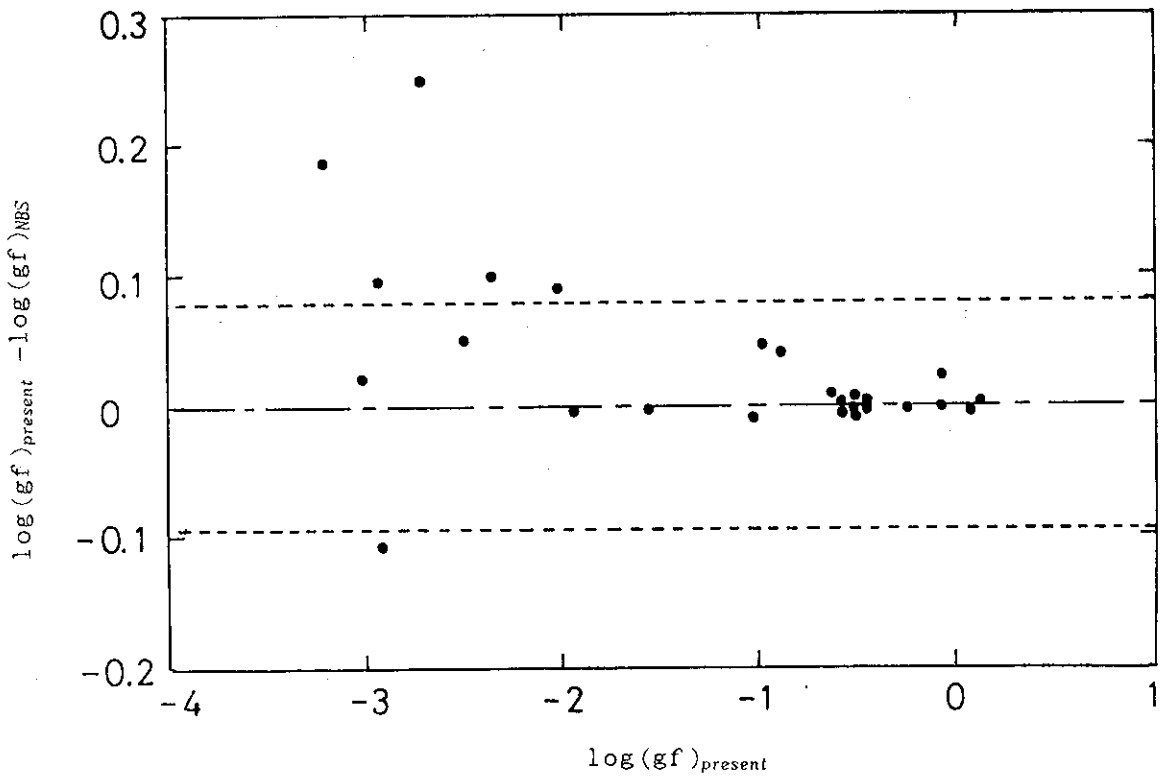

Fig.7. Plot of $\log(gf)_{present} - \log(gf)_{NBS}$ vs $\log(gf)_{present}$.